Real Coded Genetic Algorithm for Optimization of Pervaporation Process Parameters for Removal of Volatile Organics from Water

ARTICLE *in* INDUSTRIAL & ENGINEERING CHEMISTRY RESEARCH · MAY 2003

Impact Factor: 2.59 · DOI: 10.1021/ie020183t

Real Coded Genetic Algorithm for Optimization of Pervaporation Process Parameters for Removal of Volatile Organics from Water

Satyanarayana V. Suggala and Prashant K. Bhattacharya*

Department of Chemical Engineering, Indian Institute of Technology, Kanpur-208016, India

Optimal operation of the pervaporation process for the removal of multicomponent VOCs from water was studied. The data obtained were for the treatment of wastewater containing toluene, trichloroethane (TCE), and methylene chloride using poly(dimethylsiloxane) (PDMS) membrane in the form of a hollow fiber membrane module. In this study, the influence of process variables (feed composition, Reynolds number, flow rate, membrane thickness, and downstream pressure) on the module performance and process economics was studied. A population-based tool was used to optimize the process variables, and a real coded genetic algorithm was used to determine the optimum process conditions for the minimum annual wastewater treatment cost for a fixed toluene removal fraction without recycling of the permeate. It was found that the treatment cost for a multicomponent system is less than that of a single-component system at the global optimum of the process variables.

Introduction

Volatile organic compounds (VOCs) released from process industries create serious water and air-pollution problems. Conventional processes such as air stripping, carbon adsorption, chemical oxidation, incineration, etc., have been found[1] to be partially successful in removing VOCs, particularly when the concentration of the VOCs in the contaminated stream is very low and the quantity of effluent is large. Pervaporation is rapidly emerging as a viable unit operation for the separation of organic components present in water. This process not only addresses the problem of pollution, but might also recover valuable organics. The term "volatile organic compound" generally refers[2] to organic compounds that have boiling points less than 100 °C and/or vapor pressures greater than 1 mm Hg at 25 °C. Water treatment applications have been reported[3] that use of membranes made of organophillic polymers, such as silicone rubber. Such membranes exhibit high permeabilities for organic compounds while restricting the passage of water. Therefore, the concentrations of VOCs in the permeate might be orders of magnitude greater than their concentrations in the water being treated. The concentrations of VOCs in the permeate can often cross beyond their solubility limits, which might result in the separation of an aqueous and an organic phase during condensation, thus facilitating the possibility of recovering the organic fractions. Further, during pervaporation, the presence of multiple components can be advantageous because of the sharing of the downstream pressure by all components,[4] which, in turn, increases their permeation. In contrast, during carbon adsorption, the removal efficiency is reduced by competitive adsorption[5] and the limited number of activated sites for multicomponent VOCs−water mixtures.

Commercialization of a multicomponent pervaporation process requires a thorough study of many factors that affect the process performance. These include the downstream pressure, membrane thickness, Reynolds number, feed concentration, and effluent flow rate, among others. The present study was undertaken to extend the work of Ji et al.[4] in the optimization of pervaporation process variables. A shell-and-tube heat exchanger type of hollow fiber module was employed for the purpose. The feed was considered to be a mixture of toluene (Tol), 1,1,1-trichloroethane (TCE), and methylene chloride (MC) in water. Optimum parameters were estimated for 90% toluene removal without recycling of the permeate. A genetic algorithm was applied for the solution of this complex, nonlinear, multivariable optimization problem, as this technique provided a greater opportunity to obtain the true global minimum.[6] In contrast, Ji et al.[4] used Powell's technique to optimize a particular process variable (keeping other variables fixed) for a single-component system (i.e., water−toluene). Powell's method employs a single-variable search method,[7] so there is no guarantee of obtaining true global minima for multivariable problems.

Conventional optimization methods generally are associated with the following types of disadvantages: (i) exhibiting convergence dependency on the initial solution, (ii) getting stuck in suboptimal solutions, (iii) requiring a separate algorithm for each problem, (iv) being inefficient for problems with discrete search spaces, (v) being inefficient for simultaneous use on parallel machines, (vi) taking point-by-point approaches, and (vii) requiring unimodel or multimodel assumption. Genetic algorithms (GAs) overcome these disadvantages. Further, GAs are suitable for parallel implementations. In real optimization problems, most computational time is spent in evaluating solutions; with multiple processors, overall computational time can be reduced substantially.[7]

A genetic algorithms[6] represent a nontraditional search and optimization method that is finding important applications in engineering optimization. GAs mimic the principles of genetics and the Darwinian principles of natural selection (i.e., survival of the fittest). Further, each genetic algorithm is a computer simulation that operates on a constant-sized population

* To whom correspondence should be addressed. Tel.: +91-512-2597093. Fax: +91-512-2590104. E-mail: pkbhatta@iitk.ac.in.

10.1021/ie020183t CCC: $25.00
Published on Web 05/13/2003

of individuals, called the search space. The individuals in the initial population are stochastically selected, recombined, mutated, and either eliminated or retained according to their relative levels of fitness. Such algorithms find applications in problems involving discontinuities and vast search spaces with multimode noise. A simple genetic algorithm consists mainly of three operators: reproduction, crossover, and mutation. Initially, for the initial population, individuals are generated randomly. Each individual is evaluated according to a fitness function (objective function). Then, the reproduction operation is carried out by choosing individuals according to their relative fitness. High-fitness individuals are selected a greater number of times, in proportion to their relative fitness. Reproduction alone cannot introduce any new (different) individuals into a population. The crossover and mutation operations are performed to generate new individuals.

The crossover operator is believed to be the main search operator, and the purpose of this operator is twofold. Initially, random strings representing the problem variables are searched thoroughly. Beneficial portions of these strings are then combined to form potentially better strings. Thus, the crossover operation is carried out between two strings that are called "parents". Two new strings are formed by the exchange of substrings between the parents, and they are called "children". The children produced might or might not be more fit than the parents, depending on whether the crossing site falls in an appropriate place. Hence, every crossover might not create better solutions, but this does not cause a problem. If low-fitness children are created, they will be eliminated in the next reproduction operation and, hence, will have a short life. On the other hand, if high-fitness children are produced, they are likely to increase in number in the next reproduction operation. Thus, this operation tends to enable the evolutionary process to move toward "promising" regions of the search space. This is quite similar to the biological process in which complex life forms from the simple ones.[8] As an example, consider two parents that are represented by 01101011 and 00111101. If a single point crossover operation is applied with the crossover site falling at the fourth site (randomly selected) along the string length, then two children are produced as illustrated below.

The mutation operation is similar to the crossover operation and provides new individuals in the sample by changing the value of the variable. The mutation operation maintains the diversity of the sample and prevents premature convergence to local optima. Further, it creates a point in the neighborhood of the current point, thereby achieving a local search around the current solution. Each of the parents considered above has a 0 in the leftmost position. If the true optimum solution requires a 1 in that position, then neither reproduction nor crossover will be able to create a 1 in that position. In this case, the mutation operation can provide the required change by replacing the 0 in that by a 1.

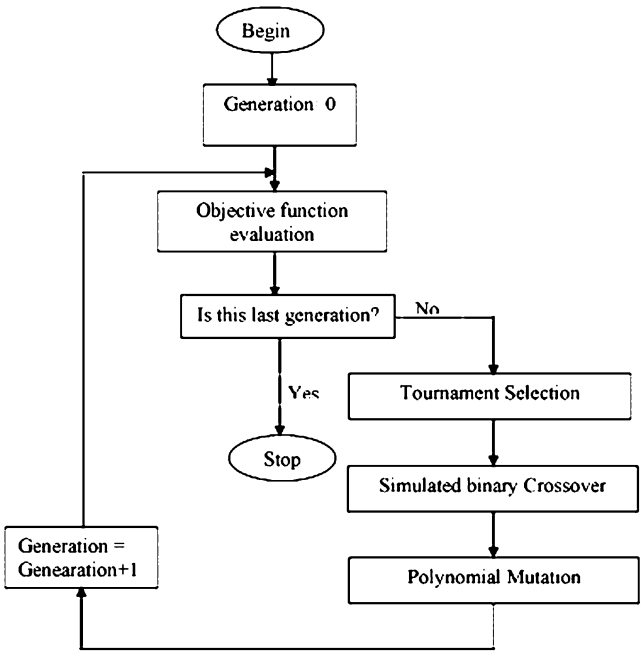

Figure 1. Flowchart of genetic algorithm.

In a binary coded genetic algorithm, the string length depends on the precision. For higher precision, the string length and population size requirements are greater,[9] thus increasing the computational complexity. Further, a fixed coding scheme is used to code the decision variables and the bounds; variable bounds must be used such that they bracket the optimum variables. In many problems, such information is not known a priori. Hence, in this work, we have used a real coded genetic algorithm. Real parameters are used directly, and optimization is easier than for binary coded GAs. However, in this case, the main problem that arises is the question of how to use a pair of real parameters to create a new pair of offspring and how to perturb a variable for the mutation. Herreara et al.[10] have provided a good overview of many real parameters used for crossover and mutation operators.

In the present work, the real coded genetic algorithm consists of the tournament selection,[11] simulated binary crossover,[12,13] and polynomial mutation[14] operators. The simple genetic algorithm flowchart is given in Figure 1. In a real coded genetic algorithm, the difference between the crossover and mutation operations lies in the number of parents used in the perturbation.[9] If only one parent is used, then it is mutation; if more than one parent is used, it is crossover. Further, perturbations are predefined in the case of mutations, and range of perturbations is adaptive in the case of crossovers.

The main objective of the present work is to apply a real coded genetic algorithm to the single-component system studied by Ji et al.[4] and compare the obtained results with values they reported and then to extend the method to multicomponent system. Further, for both types of systems, i.e., single-component and multicomponent, global optimum points were obtained.

Process Model

Mass Balance. The entire formulations, including the formulation used for the mass balance, were taken from the literature.[4] Because these formulations were developed for a single-component system, they had to be modified for multicomponent systems.

The total feed, when applied to a hollow fiber membrane module, can be divided into two flows: retentive flow and permeate flux.

The overall mass balance is given by

$$-\rho \, \mathrm{d}q = N \, \mathrm{d}A_\mathrm{m} \tag{1}$$

For each organic compound i ($i = 1, 2, ..., i$)

$$\mathrm{d}(qC_i) = -N \, \mathrm{d}A_\mathrm{m} \tag{2}$$

Rearranging eqs 1 and 2 gives

$$q \frac{\mathrm{d}C_i}{\mathrm{d}A_\mathrm{m}} = \frac{C_i N}{\rho} - N \tag{3}$$

Permeation Flux. The organic flux can be expressed[5] in terms of an overall mass-transfer coefficient

$$N_i = K_i\left(C_i - \frac{p_i}{H_i}\right) = K_i\left(C_i - \frac{py_i}{H_i}\right) \tag{4}$$

For the pervaporation of dilute solutions, the liquid boundary mass-transfer resistance for water is negligible. Hence

$$N_\mathrm{w} = L_{\mathrm{P,w}}\left(\frac{p_\mathrm{w}^\mathrm{o} - p_\mathrm{w}}{l}\right) = L_{\mathrm{P,w}}\left(\frac{p_\mathrm{w}^\mathrm{o} - py_\mathrm{w}}{l}\right) \tag{5}$$

and

$$N = \Sigma N_i + N_\mathrm{w} \qquad (\text{where } i = 1{-}3) \tag{6}$$

Overall Mass-Transfer Coefficient. According to the resistance-in-series model, the total mass-transfer resistance is the sum of the boundary-layer resistance, membrane resistance, and vapor-phase resistance. Generally, the vapor-phase resistance is negligible in comparison to the other two resistances.[15] Hence

$$\frac{1}{K_i A_\mathrm{m} l} = \frac{1}{k_{\mathrm{l},i} A_\mathrm{F} l} + \frac{1}{L_{\mathrm{P},i,\mathrm{m}} H_i A_\mathrm{m}} \tag{7}$$

For $Re < 2100$, k_l can be calculated from the Leveque equation[16]

$$Sh = 1.62 Re^{0.33} \, Sc^{0.33}\left(\frac{2r_\mathrm{i}}{L}\right)^{0.33} \tag{8}$$

For $Re > 4000$

$$Sh = 0.026 Re^{0.80} \, Sc^{0.33} \tag{9}$$

Further, eq 7 can be written as

$$\frac{1}{K_i l} = \frac{1}{k_{\mathrm{l},i} r_\mathrm{i} \ln(r_\mathrm{o}/r_\mathrm{i})} + \frac{1}{L_{\mathrm{P},i,\mathrm{m}} H_i} \tag{10}$$

Therefore

$$K_i l = \frac{L_{\mathrm{P},i,\mathrm{m}} H_i}{E_i + 1} \tag{11}$$

where

$$E_i = \frac{L_{\mathrm{P},i,\mathrm{m}} H_i}{k_{\mathrm{l},i} r_\mathrm{i} \ln(r_\mathrm{o}/r_\mathrm{i})} \tag{12}$$

Substituting eq 11 into eq 4 gives

$$N_i = \frac{L_{\mathrm{P},i,\mathrm{m}}(C_i H_i - p_i)}{(E_i + 1) l} = \frac{L_{\mathrm{P},i,\mathrm{m}}(C_i H_i - p_i)}{(E_i + 1) l} \tag{13}$$

Further, upon substitution of eqs 5, 6, and 13, eqs 1 and 3, respectively, become

$$\frac{1}{2\pi}\frac{\mathrm{d}q}{\mathrm{d}z} = -\sum_{i=1}^{3} \frac{L_{\mathrm{P},i,\mathrm{m}}}{(E_i + 1) l} \frac{(x_i H_i - py_i/\rho)}{\ln(1 + l/r_\mathrm{i})} - \frac{L_{\mathrm{P,w}}}{\rho} \frac{(p_\mathrm{w}^\mathrm{o} - py_\mathrm{w})}{\ln(1 + l/r_\mathrm{i})} \tag{14}$$

$$\frac{q}{2\pi}\frac{\mathrm{d}x_i}{\mathrm{d}z} = x_i\left[\sum_{j=1}^{3} \frac{L_{\mathrm{P},i,\mathrm{m}}}{(E_i + 1)} \frac{(x_i H_i - py_i/\rho)}{\ln(1 + l/r_\mathrm{i})} + \frac{L_{\mathrm{P,w}}}{\rho} \frac{(p_\mathrm{w}^\mathrm{o} - py_\mathrm{w})}{\ln(1 + l/r_\mathrm{i})}\right] - \frac{L_{\mathrm{P},i,\mathrm{m}}}{(E_i + 1)} \frac{(x_i H_i - py_i/\rho)}{\ln(1 + l/r_\mathrm{i})} \tag{15,16,17}$$

The above expression was obtained in terms of three equations (eqs 15−17) for $i = 1{-}3$. By solving eqs 14−17, the variation of the flow rate, the concentrations of the components along the axial direction of the fiber for a given feed flow rate, and the inlet concentrations of the components can be obtained.

Cost Model

Capital Cost. Capital cost is estimated using the Hand−Guthrie bare module method.[17] The bare module (BM) cost includes all expenses incurred in creating a working unit and all auxiliary piping, instruments, and support within the unit. This cost also includes freight duties, taxes, and engineering expenses. The major equipment required for the pervaporation process includes the membrane module, feed pump, vacuum pump, and condenser. Thus, the total capital cost can be expressed as

$$¢_\mathrm{capital} = b_\mathrm{mod}(¢_\mathrm{m} + ¢_\mathrm{mod} + ¢_\mathrm{feed\ pump} + ¢_\mathrm{vacuum\ pump} + ¢_\mathrm{condensor}) \tag{18}$$

Assuming a suggested[18] price of \$100/m^2 for a commercial hollow fiber membrane, we obtain

$$¢_\mathrm{m} = 100 A_\mathrm{m} \tag{19}$$

Similarly, a cost of \$100/m^2 for a typical hollow fiber membrane module can be taken,[5] and hence

$$¢_\mathrm{mod} = 100 A_\mathrm{m} \tag{20}$$

Further, the cost of the feed pump can be estimated[17] as

$$¢_\mathrm{feed\ pump} = 26\,700(24 \times 3600 q/50\,000)^{0.53} \tag{21}$$

Similarly, the cost of the vacuum pump can be estimated[17] as

$$¢_\mathrm{vacuum\ pump} = 4200(60 GRT_\mathrm{o}/P_\mathrm{o})^{0.55} \tag{22}$$

where T_o and P_o are standard temperature and pressure, respectively. The cost of the permeate condenser was calculated from the cost of a carbon steel shell-and-tube condenser,[17] with a condenser tube length of 3.66 m. Accordingly, for $0 < A_{condensor} < 22.30$

$$¢_{condensor} = 1176.7 + 128.1A_{condensor} \quad (23)$$

where

$$A_{condenser} = \frac{\sum_{j=1}^{4} G_j[(\Delta H)_j + C^{v}_{p,j}(\Delta T)_P]}{U(\Delta T)_F} \quad (24)$$

The value of U was taken[19] to be 9.52×10^{-3} kJ/(s·m²·K) for streams condensed by ammonia.

Treatment Cost. The treatment cost (TC) was estimated in terms of four contributions: (1) capital depreciation (CD), (2) maintenance and labor (ML), (3) membrane replacement (MR), and (4) energy consumption (EC)

$$¢_{TC} = (Fr)_{CD}¢_{capital} + (Fr)_{ML}¢_{capital} + ¢_{MR} + ¢_{EC} \quad (25)$$

To cover depreciation and taxes (CD), a value[19] of 15% of the installed total capital cost was assumed. The annual maintenance and labor costs were taken[19] to be 10% of the total capital cost. Further, a membrane life of 3 years[18] was assumed. Therefore

$$¢_{MR} = 100A_m/3 \quad (26)$$

Energy is consumed to pump the feed, run the vacuum pump, and condense the vapor. Therefore

$$¢_{EC} = et\left(\frac{W_F}{\eta_F} + \frac{W_{vacuum}}{\eta_{vacuum}} + \frac{W_{condensor}}{\eta_{condensor}}\right) \quad (27)$$

where W_F is the power of the feed pump, which was taken[20] as the product of flow rate q and the flow pressure drop Δp

$$W_F = q\Delta p \quad (28)$$

In pervaporation, the downstream pressure is maintained by efficient condensation of the permeate. The condensation temperature controls the downstream pressure. Because of the limited solubility of organics in water, the permeate can be obtained in two phases. Further, it was assumed that equilibrium was reached among organic and aqueous phases. Therefore

$$f_i^v = f_i^l \quad (29)$$

$$\Sigma p_i(T) = \Sigma p_i^o \gamma_i^\infty x_i = \Sigma p_i^o y_i^{org} \quad (30)$$

$$p_w \approx p_w^o \quad (31)$$

$$p = \sum_i p_i(T) + p_w(T) \approx \sum_i p_i^o(T) y_i^{org} + p_w^o(T) \quad (32)$$

A vacuum pump was used to remove the inert gas, and it was assumed to operate for 10% of the total operating time. The work done by the vacuum pump is therefore

$$W_{vaccum} = 0.1G\frac{k}{k-1}RT[(P_o/p)^{(k-1/k)} - 1] \quad (33)$$

Further, the energy balance on the condenser gives the energy consumption

$$W_{condensor} = \sum_{j=1}^{4}[G_j((\Delta H)_j + C^{v}_{p,j}(\Delta T)_P)] \quad (34)$$

Hence, all of the cost equations (eqs 18−34, excluding 25) along with the standard data were substituted into eq 25 to obtain the treatment cost equation. Therefore, in eq 25, the treatment cost becomes a function of the inlet flow rate, the Reynolds number, the downstream pressure, the permeate flow rate, and the membrane area. Further, the membrane area and permeate flow rate are functions of the membrane thickness, feed concentration, downstream pressure, Reynolds number, and removal fraction (defined as the concentration difference between the inlet and outlet of the module divided by the inlet concentration). The single objective treatment cost equation thus obtained was minimized.

It should be stated at this point that, according to Deb,[9] if a relative preference among the objectives is known for a specific problem, there is no need to formulate and solve a multiobjective optimization problem. A simple weighted sum approach can be adopted for such cases. Therefore, a single objective function was utilized for the present work, as the main objective was to study the optimization of process variables for a multicomponent system. However, one could attempt to solve a multiobjective function to find multiple pareto-optimal solutions, depending on the situation. For example, if one of the costs were more significant or dominant than the others (such as the energy over other costs, which might be relevant depending on the availability of exact membrane plant data, geographical location, etc.), then a multiobjective approach can be applied.

Solution Method and Optimization

The main objective is to minimize the treatment cost subject to the operating variables (q, Re, l, p, x_i) having the following selected minimum and maximum values:

$$2.77 \times 10^{-3} < q < 5.77 \times 10^{-3}$$

$$20 < Re < 7000$$

$$5 \times 10^{-6} < l < 10^{-4}$$

$$0.2 < p < 4.0$$

$$2 \times 10^{-6} < x_{Tol} < 9.8 \times 10^{-5}$$

$$2 \times 10^{-6} < x_{TCE} < 9.7 \times 10^{-5}$$

$$2 \times 10^{-6} < x_{MC} < 4.01 \times 10^{-3}$$

The minimum and maximum values were chosen so that the values below and above them are practically insignificant during pervaporation. For example, the maximum toluene concentration chosen in the effluent is the solubility limit of toluene in water, i.e., 500 ppm ($x_{Tol} = 9.8 \times 10^{-5}$). A poly(dimethylsiloxane) membrane was chosen for the separation, and the permeabilities of different species through this type of membrane were

Table 1. PDMS Membrane Permeability for Feed Components[3] [a]

compound	permeability [10^{-8} mol·m/(m^2·kPa·s)]
toluene	5.28
trichloroethane	1.58
methylene chloride	1.82
water	2.32

[a] Temperature = 30°C.

Table 2. Physical Properties of Feed Components[a]

compound	heat capacity [J/(mol·K)]	heat of vaporization (kJ/mol)	Henry's constant (kPa·m^3/mol)	diffusion coefficient (10^{-9} m^2/s)
toluene	157.44	37.56	0.7358	1.97
1,1,2-trichloroethane	145.09	37.65	2.1115	2.56
methylene chloride	128.35	28.54	0.1181	2.57
water	34.25	43.76		

[a] Temperature = 30°C.

taken from the literature,[3] as listed in Table 1. A toluene removal fraction of 0.9 was assumed. Binary diffusion coefficients of organic components in water were estimated[21] from the Wilke−Chang equation and are given in Table 2. Vapor pressures were calculated[22] from Antoine's equation.

Calculation of the treatment cost requires the membrane area and the total and individual permeate fluxes. Differential eqs 14−17 were solved by a fourth-order Runga−Kutta method.[23] However, evaluation of the right-hand sides of the differential equations required permeate compositions, which were calculated by dividing eq 4 by eq 5 and using $\sum y_i = 1$. The resulting algebraic equations were solved using the Newton−Raphson technique,[23] considering hollow fiber module to be series of mixed elements. Accordingly, the permeate stream composition and permeate flow rate were calculated for each element. Further, the mass balance equations were used to obtain the feed stream composition of the second element. This procedure was repeated until a 90% reduction of toluene concentration was achieved. Then, to optimize the process variables, a real coded genetic algorithm was used. The bounds of the variables were directly specified in genetic algorithm program. The computations were performed on a Linserv, Red Hat 7.0 release, modified UNIX operating system (useful for parallel programming under Linux with the specifications Proliant ML350 P III, 800-MHZ processor, dual CPUs, 128 MB RAM). The CPU time was around 4 h.

Results and Discussion

Genetic Algorithm Parametric Study. Genetic algorithms are stochastic optimization techniques. The population size, crossover probability, mutation probability, and random seed all can affect the optimum values. Figure 2a−d shows the effects of these parameters on the optimized Reynolds number in a multicomponent system. These plots (Figure 2a−d) are depicted for the optimized Reynolds number as a function of population size, crossover probability, mutation probability, and random seed, respectively. It is clear that these variables do not affect the optimized Reynolds number. However, there is a marginal effect of the population size on the Reynolds number. As the population size increases, the optimum Reynolds number also increases. Generally, it is believed[9] that larger population sizes will provide better optimum results. Harika et al.[24] provided certain general steps for the selection of population size. It can be further observed from Figure 2d that, as the random seed changes from 0.123 to 0.500, the optimum Reynolds number varies, but only by a marginal amount. This study clearly shows that the GA parameters do not have much of an effect on the optimum value obtained for this optimization problem. Therefore, fixed GA parameters were used for the present work. The parameter values used for the study are given in Table 3. Previously,[25,26] fixed GA parameters have also been used to solve chemical engineering optimization problems. However, caution must be taken, even for simpler problems, that any arbitrary choice of parameter settings might not necessarily work well. Qi and Palmieri[27] systematically studied the effect of GA parameters on different problems.

System Containing a Single Organic Component. Optimization of the process variables for a system containing a single organic component using real coded genetic algorithm was carried out, and the results were compared to the values obtained by Ji et al.[4] Figure 3 shows the effect of the Reynolds number on the treatment cost for 90% toluene removal from a 500 ppm feed toluene solution using a module with a fiber diameter of 100 μm. The optimum Reynolds number was estimated to be 230, close to the value of 250 obtained by Ji et al.[4] The difference might be due to the new optimization technique and the properties used. For the full range of *Re* studied, refer to the inset of Figure 3. Figure 4 shows the effect of the Reynolds number on the treatment cost in the turbulent region. The treatment cost increases with increasing Reynolds number in this region, which might be due to an increase in the feed pumping costs. The global optimum was found in the laminar region. Similar conclusions were also drawn by Ji et al..[4] The distributions of various costs at the optimum points obtained are reported in Table 4. Figure 5 shows the effect of the Reynolds number on the treatment cost for a fiber diameter of 400 μm. As the fiber diameter is increased, the liquid-film mass-transfer coefficient decreases, and the membrane area increases. In this case, the global optimum is shifted into the turbulent region. These results were also similar to the earlier-obtained[4] results. The effect of the feed flow rate on the specific treatment cost is shown in Figure 6. The specific treatment cost decreases slightly with increasing feed flow rate, which confims the earlierobservations.[4] Figure 7 shows the effect of the feed toluene concentration on the treatment cost. The treatment cost increases marginally with increasing feed concentration.

Global Optimum. For analysis of the global optimum, all process variables were varied simultaneously. The results obtained at global points are reported in Table 4. It was observed that the capital cost and feed pumping cost dominated the total treatment cost. Hence, the total cost appears to be sensitive to the assumptions about costs made for the module, equipment, pumping efficiency, and electricity. The distribution of the costs for this system is shown in Figure 8 in the form of a pie chart.

Multicomponent System. Optimization of the process variables for a multicomponent system consisting of toluene, trichloroethane, and methylene chloride was carried out at 90% toluene removal with a hollow fiber diameter of 100 μm.

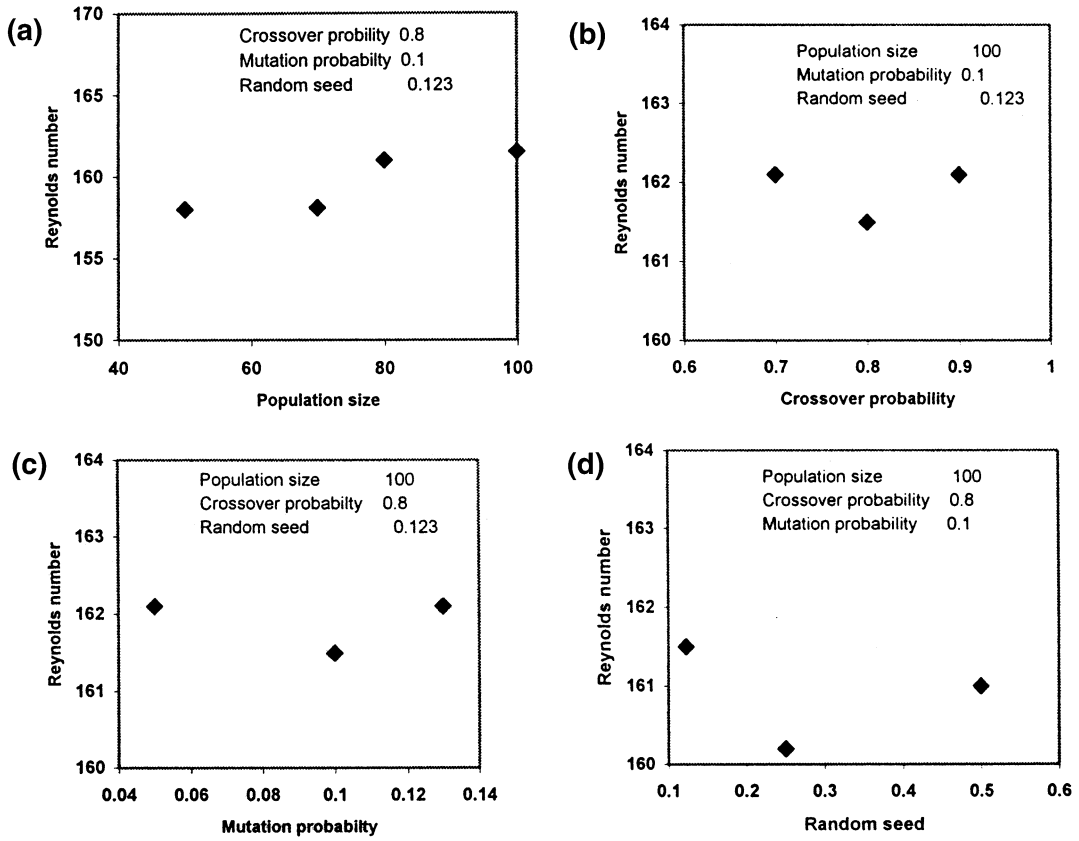

Figure 2. Effect of genetic algorithm parameters on Reynolds number in multicomponent system.

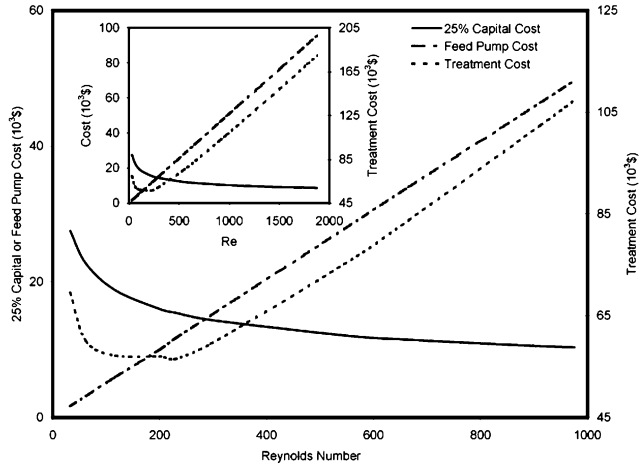

Figure 3. Effect of Reynolds number on cost under laminar flow for system with a single organic component (at $q = 16$ m^3/h, $l = 25$ μm, $p = 1$ kPa, $x_{Tol} = 500$ ppm, $r_i = 100$ μm).

Table 3. Selected Computational Parameters of Real Coded Genetic Algorithm

no. of variables	7
population size	100
maximum no. of generations	50
distribution index for crossovers	10
distribution index for mutations	10
crossover probability	0.800
mutation probability	0.100
random seed	0.123

Influence of the Feed-Side Reynolds Number. The effect of the feed-side Reynolds number on the process economics is shown in Figure 9 for fixed values of the other variables. It can be seen that the treatment cost (25% of capital plus pumping costs, etc.) initially

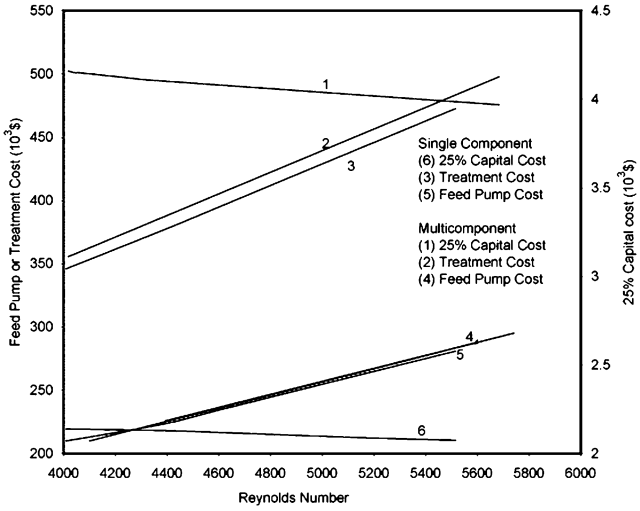

Figure 4. Effect of Reynolds number on cost under turbulent flow (at $q = 16$ m^3/h, $l = 25$ μm, $p = 1$ kPa, $x_{Tol} = 500$ ppm, $r_i = 100$ μm).

decreases with increasing *Re*; however, soon, this cost sharply increases with increasing *Re*. Hence, a minima is observed at *Re* of 161. This can be attributed to the fact that, as *Re* increases, the mass-transfer coefficient in the liquid boundary layer increases, which increases the overall mass transfer for a given membrane. Therefore, for a fixed removal fraction of toluene, the membrane area decreases. This decrease in membrane area decreases the capital cost. However, the feed pumping cost increases rapidly because of the increase in pressure losses, so, the operating cost increases. These two opposing trends result in an optimal Reynolds number value of 161.5. For the full range of *Re* studied, refer to

Table 4. Estimated Costs at Optimum Points[a] with Other Variables Fixed

							costs (10^3 $)				
q (10^{-3} m^3/s)	Re	l (μm)	P (kPa)	x_{Tol} (ppm)	x_{TCE} (ppm)	x_{MC} (ppm)	25% capital	membrane	condensation + vacuum	feed pump	treatment
4.444	**231.0**	25	1.00	500.0	0	0	1.55	5.047	16.70	19.7	57.07
1.397	**191.9**	**62**	**3.16**	**360.8**	**0**	**0**	6.26	3.307	1.50	5.1	16.25
4.444	**161.5**	25	1.00	500.0	720.0	19 400	22.32	5.535	31.05	13.8	72.74
4.444	**4009.8**	25	1.00	500.0	720.0	19 400	4.16	3.004	6.84	343.5	354.88
4.444	161.5	**84**	1.00	500.0	720.0	19 400	22.21	8.068	19.58	13.7	62.66
4.444	161.5	84	**4.00**	500.0	720.0	19 400	19.45	5.835	20.03	13.7	59.12
1.444	**121.2**	**95**	**1.78**	**351.6**	**399.3**	**2698**	6.64	3.179	2.80	3.3	15.99

[a] Optimum points indicated by bold numerals.

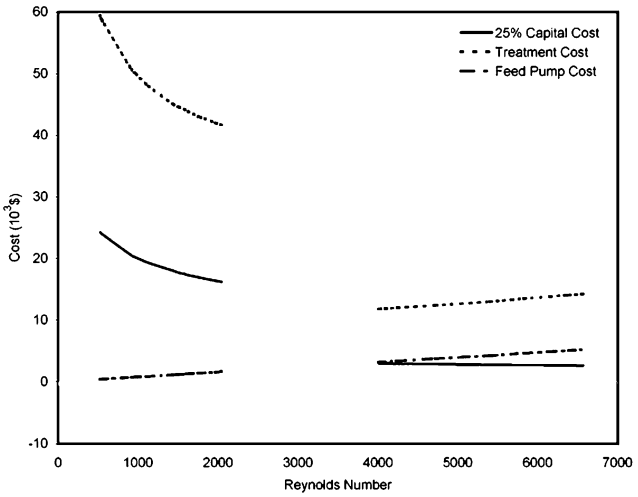

Figure 5. Effect of Reynolds number on cost under different flow regimes for a 400-μm fiber diameter (at $q = 16$ m^3/h, $l = 25$ μm, $p = 1$ kPa, $x_{Tol} = 500$ ppm, $r_i = 400$ μm).

the inset of Figure 9. Further, Figure 4 shows the variation of the treatment cost in the turbulent region. In the turbulent region, the mass-transfer coefficients are very high, which causes the membrane area and capital cost requirements to decrease. However, the increase in Reynolds number increases the cost of pumping the feed tremendously. Subsequently, therefore, the treatment cost increases sharply. Hence, the global optimum was found to be in the laminar region. In this study, binary diffusion coefficients were used to study the process economics. Use of diffusion coefficients in multicomponent mixtures might further reduce the optimum Reynolds number because of the similar natures of organic components.

Influence of the Membrane Thickness. Process economics are greatly affected by the membrane thickness. Organic compounds have a high affinity for silicone rubbers. With these types of polymers, the liquid film resistance might be the rate-limiting step. As a result, for poor hydrodynamic conditions, the thickness of silicone rubber might have little effect on the organic flux, whereas there might be a significant reduction of the water flux. The effect of the membrane thickness on the treatment cost is shown in Figure 10. It is observed that, initially, the treatment cost decreases significantly with increasing membrane thickness, whereas the cost attains a plateau at higher thickness (refer to the inset of Figure 10). This can be explained by the fact that the flux is higher with thinner membranes. This reduces the membrane area and the capital cost for a given separation. However, the treatment cost becomes higher because of the high energy costs for vapor pumping and condensation. Further, from Table 4, it can be observed that the cost of condensation and vapor pumping ($19,580) is larger than the other treatment costs (membrane cost = $8,068). Hence, the treatment cost is more sensitive to the condensation

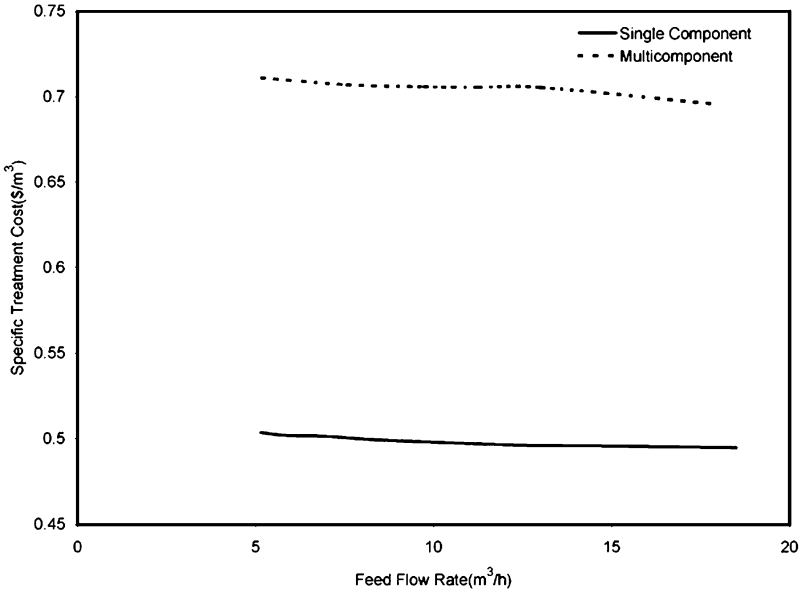

Figure 6. Effect of feed flow rate on specific unit treatment cost (conditions for single-component system, $Re = 230$, $l = 25$ μm, $p = 1$ kPa, $x_{Tol} = 500$ ppm, $r_i = 100$ μm; conditions for multicomponent system, $Re = 161$, $l = 84$ μm, $p = 4$ kPa, $x_{Tol} = 500$ ppm, $x_{TCE} = 720$ ppm, $x_{MC} = 19\,400$ ppm, $r_i = 100$ μm).

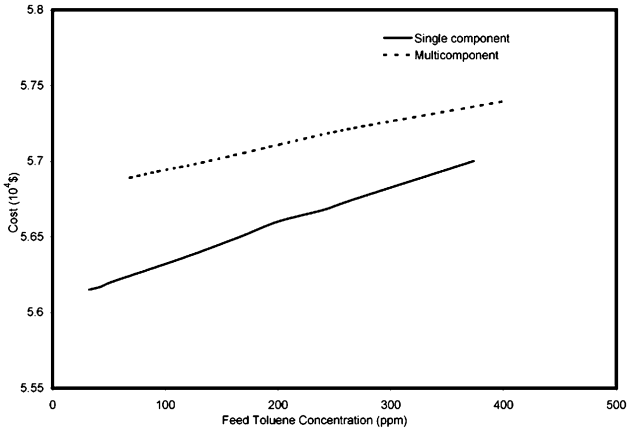

Figure 7. Effect of toluene feed concentration on treatment cost (Re = 230, q = 16 m^3/h, l = 25 μm, p = 1 kPa, r_i = 100 μm; conditions for multicomponent system, Re = 161, q = 16 m^3/h, l = 84 μm, p = 4 kPa, x_{TCE} = 720 ppm, x_{MC} = 19 400 ppm, r_i = 100 μm).

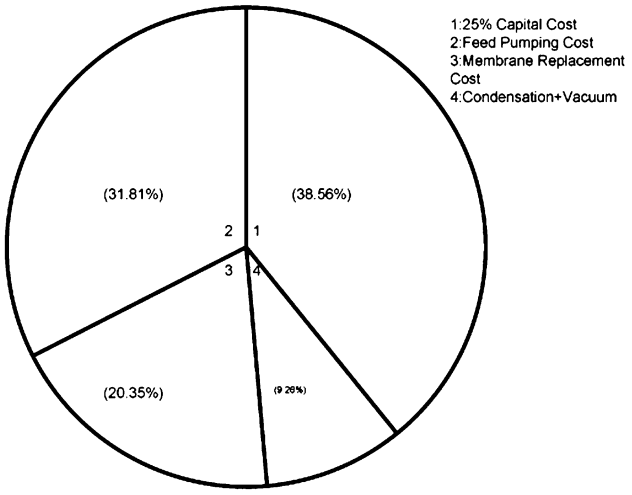

Figure 8. Distribution of various costs at global optimum point for single-component system.

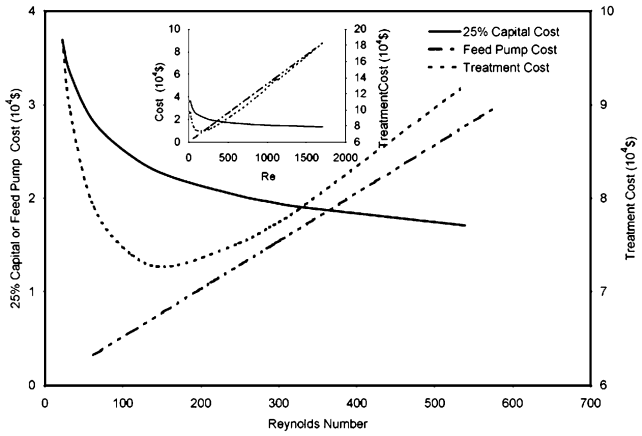

Figure 9. Effect of Reynolds number on cost under laminar flow for multicomponent system (at q = 16 m^3/h, l = 25 μm, p = 1 kPa, x_{Tol} = 500 ppm, x_{TCE} = 720 ppm, x_{MC} = 19 400 ppm, r_i = 100 μm).

cost. A decrease in the thickness of the membrane increases the treatment cost, and to some extent, an increase in the membrane thickness decreases the treatment cost. Therefore, there should be an optimum membrane thickness. Such an optimization calculation provided a membrane thickness of 84 μm. This value is

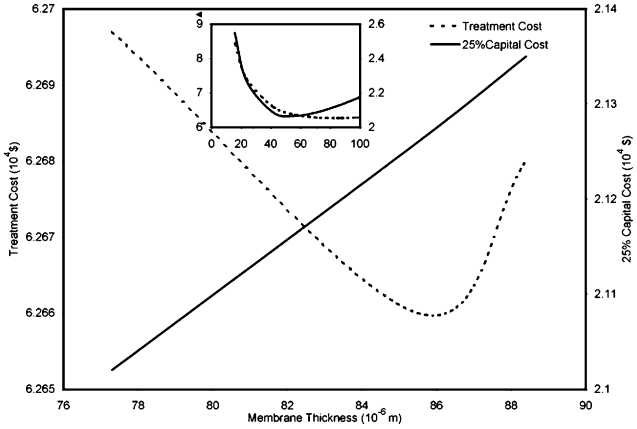

Figure 10. Effect of membrane thickness on cost for multicomponent system (at Re = 161, q = 16 m^3/h, p = 1 kPa, x_{Tol} = 500 ppm, x_{TCE} = 720 ppm, x_{MC} = 19 400 ppm, r_i = 100 μm).

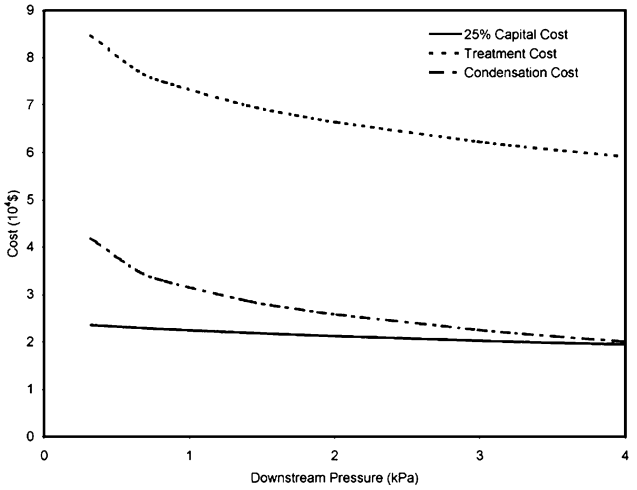

Figure 11. Effect of downstream pressure on cost for multicomponent system (at Re = 161, q = 16 m^3/h, l = 84 μm, x_{Tol} = 500 ppm, x_{TCE} = 720 ppm, x_{MC} = 19 400 ppm, r_i = 100 μm).

much larger than the membrane thickness of the single-component system studied (25 μm).[4] The total treatment cost appears to be more sensitive to the condensation energy for multicomponent systems, which might have resulted in a high optimum thickness. The reason behind our earlier discussion for the case of a higher membrane thickness is that the condensation cost is less for multicomponent systems.

Influence of the Downstream Pressure. The effect of the downstream pressure on the process economics is shown in Figure 11. It can be seen that treatment cost decreases continuously with increasing downstream pressure. This might be because, as the downstream pressure increases, both the water and the organic fluxes decrease with an increase in the selectivity.[3] Thus, with an increase in the downstream pressure, for a fixed removal fraction of toluene, there might be a marginal increase in the membrane area, capital cost, and membrane replacement cost. However, on other side, the sum of the vacuum pumping and condensation energy costs decreases significantly. These two opposite trends result in an optimum pressure of 4 kPa, which is highest permissible downstream pressure. Further, in multicomponent systems, the total downstream pressure is shared by all of the components; thus, the driving force for a particular component increases, and this reduces the membrane area requirement. Hence, the

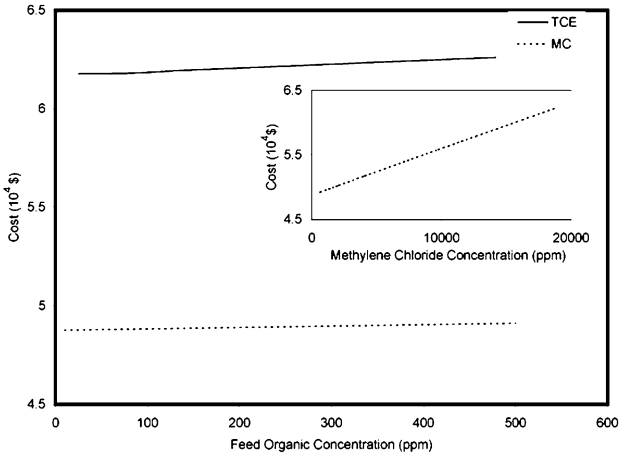

Figure 12. Effect of feed organic concentration on treatment cost (at $Re = 161$, $q = 16$ m^3/h, $l = 84$ μm, $p = 4$ kPa, $x_{Tol} = 720$ ppm, $r_i = 100$ μm).

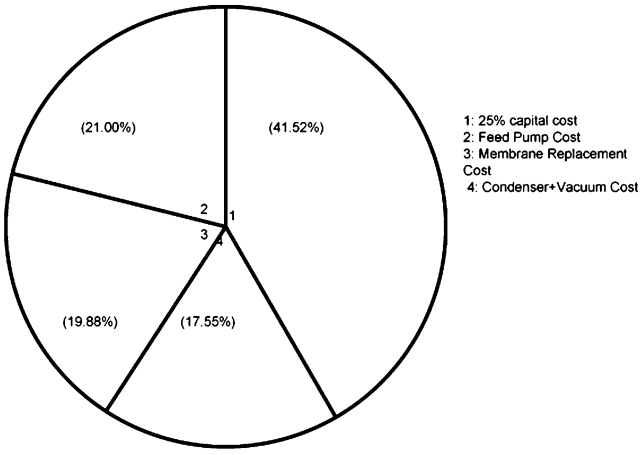

Figure 13. Distribution of various costs at global optimum point for multicomponent system.

membrane replacement cost becomes less than that for a single-component system. However, on the other hand, the cost of condensation increases, as other permeating components also need to be removed. Moreover, from Table 4, it can be observed that the treatment cost is more sensitive to the condensation energy; hence, a relatively high optimum pressure of 4 kPa was obtained for the multicomponent system studied as compared to 1.6 kPa for the single-component[4] system.

Sensitivity Analysis. The feed concentration and quantity of effluent can vary considerably depending on the source of the waste stream. thus, it was considered necessary to study the effects of these parameters on the process economics. Figure 6 also shows the effect of the feed flow rate on the specific unit treatment cost (treatment cost per cubic meter of flow rate) for the optimum values of the variables. It is evident that the specific treatment cost decreases slightly with increasing feed flow rate. Therefore, one can infer that the process of pervaporation might be more economical in dealing with larger waste stream flow rates. Further, it can also be observed from the graph that the increase in specific treatment cost is around \$0.2/m^3 for the multicomponent system compared to the system with a single organic component.

Further, the sensitivity of the treatment cost with respect to the feed toluene concentration (at 90% toluene removal) is shown Figure 7. This graph shows that there is a marginal increase in cost (~\$500), and hence, the optimal treatment cost can be considered to be independent of the feed concentration. Similar types of results were also obtained for the single-component system. Further, from Figure 7, it can be observed that, for a fixed removal fraction of toluene, the total treatment cost is almost same. Therefore, the presence of other components might not affect the process economics. In a sense, it can be concluded that the process of pervaporation might be more economical for treating systems having multiple components as compared to the process of adsorption. In the case of adsorption, the presence of other components generally decreases the number of adsorption sites, and this increases the treatment cost. Figure 12 shows that there is a marginal effect on the treatment cost of increasing the concentration of TCE in the feed for 90% toluene removal. A similar trend can also be observed for methylene chloride between 10 and 500 ppm concentrations. However, the effect of the methyelne chloride concentration, beyond 10−19 400 ppm, on the treatment cost for 90% toluene removal is also shown in the inset of Figure 12. There is now a linear increase in the treatment cost, although it is not significant. This might result from the increase in the flux of methylene chloride, which increases its concentration in feed and, hence, also increases the condensation and treatment costs.

Global Optimum. The next objective of our study was to find the global optimum for the multicomponent system by varying all variables simultaneously. The distribution of the various costs at the global optimum point is shown in Figure 13. Table 4 lists the optimum values of variables for the multicomponent system and various costs associated with the optimum points. From this table, it is clear that the treatment cost for the multicomponent system is less than that of the single-component system at optimum point. This verifies that the separation of the multicomponent system by the pervaporation process might be more economical. This finding is in contrast to the conventional separation process of adsorption and air stripping, where the treatment cost is more for multicomponent systems. Further, the pervaporation process does not require any chemical reagents and/or regeneration of an absorbent. Unlike air stripping, it does not create any other pollution problems. Moreover, in pervaporation, the removal efficiency is essentially a function of the affinity of the organic compounds for the polymeric membrane. A wide variety of polymers can, therefore, be used for a given separation.

Conclusions

An available[4] formulated optimized problem was solved to obtain process variables using a real coded genetic algorithm for the previously studied single-component system. The problem was further extended to a multicomponent system for the same purpose. The solution provided the optimum process conditions for the minimum annual treatment cost of wastewater. It was observed that the global optimum existed in the laminar region. Further, studies on the effects of process variables on the cost showed that, for a fixed removal fraction of toluene, the treatment cost was not significantly affected by the toluene concentration or the presence of other components. The thickness of the selected PDMS membrane, a rubbery polymer (provid-

ing a high organic flux), exhibited little influence on the cost as compared to the Reynolds number. Still, a value of 84 μm was obtained as the optimum thickness. In the multicomponent system, as total downstream pressure was shared by all components, it was observed that a low vacuum was required. Further, the specific treatment cost decreased slightly with increasing feed flow rate. The distributions of various costs at the global optimum points of the single- and multicomponent systems were found. The total treatment cost at the optimum point was estimated to be less for the multicomponent system than for the single-component system.

Notation

A = area (m^2)
b = module factor
C = concentration ($kmol/m^3$)
C_p = specific heat capacity [kJ/(kmol·K)]
D = diffusivity (m^2/s)
E = dimensionless number
e = price of electricity ($/kWh)
f = fugacity (kPa)
Fr = fraction
G = total permeate flow (kmol/s)
H_i = Henry's law constant of component i (kPa·m^3/mol)
H = enthalpy (kJ/kmol)
N = permeation flux [kmol/(m^2·s)]
K = overall mass-transfer coefficient (m/s)
k_l = mass-transfer coefficient in the boundary layer (m/s)
k = heat capacity ratio
L = length of hollow fiber (m)
L_P = permeability [kmol·m/(m^2·kPa·s)]
l = membrane thickness (m)
MC = methylene chloride
p = downstream pressure (kPa)
$p°$ = saturation vapor pressure (kPa)
ΔP = feed-side pressure drop (kPa)
q = feed flow rate (m^3/s)
r_i = inner radius of the hollow fiber (m)
r_o = outer radius of the hollow fiber (m)
R = universal gas constant [J/(mol·K)]
Re = Reynolds number
Sc = Schmidt number
Sh = Sherwood number
T = temperature (K)
TCE = trichloroethane
Tol = toluene
t = time period (h)
U = overall heat-transfer coefficient [kJ/(s·m^2·K)]
W = energy consumption (kW)
x = mole fraction at the feed side
y = mole fraction at the permeate side
z = axial coordinate

Greek Symbols

γ = activity coefficient
ρ = total concentration of the feed ($kmol/m^3$)
Δ = difference
μ = viscosity [kg/(m·s)]
η = efficiency factor
$\not\in$ = cost ($)

Subscripts

F = feed side
i = organic compounds (i = 1−3)
j = compounds (j = 1−3 and water)
m = membrane
mod = module
P = permeate side
w = water

Superscripts

l = liquid phase
org = organic phase in permeate
v = vapor phase

Literature Cited

(1) Brown, J. J.; Erickson, M. D.; Beskid, N. J. Applying Membrane Technology to Air Stripping Effluent for Remediation of Ground Water Contaminated with Volatile Organic Compounds. *Hazard. Waste Hazard. Mater.* **1993**, *10*, 335−345.

(2) Metcalf & Eddy, Inc. *Wastewater Engineering: Treatment, Disposal and Reuse*, 3rd ed.; McGraw-Hill: New York, 1991.

(3) Ji, W.; Sikdar, S. K.; Hwang, S. T. Modeling of Multicomponent Pervaporation for Removal Volatile Organic Compounds from Water. *J. Membr. Sci.* **1994**, *93*, 1.

(4) Ji, W.; Hilaly, A.; Sikdar, S. K.; Hwang, S. T. Optimization of Multi-component Pervaporation for Removal of Volatile Organic Compounds from Water. *J. Membr. Sci.* **1994**, *97*, 109−125.

(5) Lipsi, C.; Cote, P. The Use of Pervaporation for the Removal Organic Contaminants from Water. *Environ. Prog.* **1990**, *9*, 254.

(6) Goldberg, D. E. *Genetic Algorithms in Search, Optimization and Machine Learning*; Addison-Wesley: Reading, MA, 2000.

(7) Deb, K. *Optimization for Engineering Design*; Prentice Hall of India: New Delhi, India, 2000.

(8) Dawkins, R. *The Selfish Gene*; Oxford University Press: New York, 1976.

(9) Deb, K. *Multi-objective Optimization Using Evolutionary Algorithms*; John Wiley & Sons: New York, 2001.

(10) Herrera, F.; Lozano, M.; Verdegay, J. L. Tackling Real Coded Genetic Algorithms: Operators and Tools for Behavioural Analysis. *Artif. Intell. Rev.* **1998**, *12* (4), 265−319.

(11) Goldberg, D. E.; Deb, K. A Comparison of Selection Schemes used in Genetic Algorithms. In *Foundations of Genetic Algorithms*; Rawlins, G. J. E. Ed.; Morgan Kauffman: San Diego, CA, 1990; Vol. 1, pp 69−93.

(12) Deb, K.; Agrawal, R. B. Simulated Binary Crossover for Continuous Search Space. *Complex Syst.* **1995**, *9* (2), 115−148.

(13) Deb, K.; Kumar, A. Real Coded Genetic Algorithms with Simulated Binary Crossover: Studies on Multi-modal and Multi-objective Problems. *Complex Syst.* **1995**, *9* (6), 431−454.

(14) Deb, K.; Agrawal, S. A Niched-Penalty Approach for Constraint Handling in Genetic Algorithms. In *Proceedings of the International Conference on Artificial Neural Networks and Genetic Algorithms*; Albrecht, R., Dobnikar, A., Pearson, D., Steele, N., Eds.; Springer-Verlag: New York, 1999; pp 235−243.

(15) Meuleman, E. E. B.; Bosch, B.; Mulder, M. H. V.; Strathmann, H. Modelling of Liquid/Liquid Separation by Pervaporation: Toluene from Water. *AIChE J.* **1999**, *45*, 2153−2160.

(16) Cussler, E. L *Diffusion: Mass Transfer in Fluid Systems*; Cambridge University Press: NewDelhi, 1998 (First South Asian Edition).

(17) Woods, D. R. *Cost Estimation for the Process Industry*; McMaster University: Hamilton, Ontario, Canada, 1983.

(18) Blume, I.; Wijmans, J. G.; Baker, R. W. The Separation of Dissolved Organics from Water by Pervaporation. *J. Membr. Sci.* **1990**, *36*, 463.

(19) Peter, M. S.; Timmerhouse, *K. D. Plant Design and Economics for Chemical Engineers*; McGraw-Hill: New York, 1990.

(20) McCabe, W. L.; Smith, J. M.; Harriott, P. *Unit Operations of Chemical Engineering*; McGraw-Hill: New York, 1985.

(21) Trybal, R. E. *Mass-Transfer Operations*, 3rd ed.; McGraw-Hill: New York, 1986.

(22) Himmelblau, D. M. *Basic Principles and Calculations in Chemical Engineering*; Prentice Hall of India: New Delhi, India, 1995.

(23) Gupta, S. K. *Numerical Methods for Engineers*; New Age International: New Delhi, India, 1995.

(24) Harik, G.; Cantu-Paz, E.; Goldberg, D. E.; Miller, B. L. The Gambler's Ruin Problem, Genetic Algorithms, and the Sizing of Populations. *Evol. Comput. J.* **1999**, *7* (3), 231−254.

(25) Chan, C. Y.; Aatmeeyata.; Santosh, K. G.; Ajay, K. R. Multi-Objective Optimization of Membrane Separation Modules Using Genetic Algorithms. *J. Membr. Sci.* **2000**, *176*, 177−196.

(26) Ravi, G.; Santosh, K. G.; Viswanathan, S.; Ray, M. B. Optimization of Venturi Scrubbers Using Genetic Algorithm. *Ind. Eng. Chem. Res.* **2002**, *41*, 2988−3002.

(27) Qi, X.; Palmieri, F. Adaptive Mutation in Genetic Algorithms. In *Proceedings of the Second Annual Conference on Evolutionary Programming*; Atmar, W., Fogel, D., Eds.; Evolutionary Programming Society: La Jolla, CA, 1993; pp 192−196.

Received for review March 11, 2002
Revised manuscript received March 18, 2003
Accepted April 8, 2003

IE020183T